Int. J. Solids Structures Vol. 23, No. 10, pp. 1435–1446, 1987
Printed in Great Britain.

0020-7683/87 $3.00+ .00

EFFECT OF MATERIAL PARAMETERS ON THE INITIATION AND GROWTH OF ADIABATIC SHEAR BANDS

R. C. BATRA
Department of Engineering Mechanics, University of Missouri–Rolla, Rolla, MO 65401-0249, U.S.A.

(*Received* 3 *December* 1986; *in revised form* 14 *April* 1987)

Abstract—The thermomechanical problem involving simple shearing of a finite slab made of an isotropic and viscoplastic material is studied with the objective of finding the effect of the strain hardening parameter, strain-rate hardening parameters, thermal softening coefficient and thermal conductivity on the initiation and growth of adiabatic shear bands. The body is placed in a hard loading device, i.e. the velocity is prescribed at its top and bottom surfaces. A shear band is presumed to have formed if the addition of a perturbation in the temperature at the onset of plastic flow results in a localization of the shear strain. The critical strain at which the band begins to form is found and its dependence on various material parameters is investigated.

INTRODUCTION

In 1944 Zener and Hollomon[1] recognized the destabilizing effect of thermal softening in reducing the slope of the stress–strain curve in nearly adiabatic deformations. They postulated that a negative slope of the stress–strain curve implies an intrinsic instability of the material. Thus the strain at which the shear strain localization may initiate corresponds to the peak in the stress–strain curve. They observed 32 μm wide shear bands in a steel plate punched by a standard die and estimated the maximum strain in the band to be 100. Recht[2], assuming that the instability occurs at the peak in the stress–strain curve and this curve is independent of the strain rate, derived values of strain rate necessary to produce shear strain localization and compared these values for different materials. Staker[3] used the same instability criterion but included the dependence of the flow stress upon strain rate also. Assuming parabolic strain and strain-rate hardening laws, he concluded that important material parameters are the specific heat, slope of the temperature dependence of the flow stress, and parameters indicating the strain hardening capacity of the material. The thermal conductivity, yield strength and strain-rate sensitivity do not enter in as a first-order effect.

Instead of presuming that the material becomes unstable at a stress maximum, Clifton[4] and Bai[5] studied the growth of infinitesimal periodic perturbations superimposed on a body deformed by a finite amount in simple shear. Both investigators included the effect of strain hardening, strain-rate sensitivity, thermal softening and heat conduction. Bai also included the effect of inertia forces. Bai's instability criterion is essentially insensitive to strain-rate hardening parameters and for a parabolic type strain hardening material gives the same value of critical strain as that derived by Staker[3]. Burns[6] used a dual asymptotic expansion to account for the time dependence of the homogeneous solution in the analysis of the growth of superimposed infinitesimal perturbations. He showed that the growth rate of small perturbations is controlled by the ratio of the slope of the homogeneous stress vs strain curve to the rate of change of the plastic flow stress with respect to the strain rate. However, this growth rate was not large enough for Litonski's[7] constitutive relation to account for the experimental observations of Costin *et al.*[8]. Costin *et al.* observed 370–500 μm wide shear bands during dynamic torsion tests involving strain rates of 500 s^{-1} on short specimens of 1018 cold-rolled steel. Similar observations on twelve ductile materials have been reported by Johnson *et al.*[9] and Lindholm and Johnson[10].

Merzer[11], by using a material model due to Bodner and Partom[12], studied the problem of twisting of a thin tubular specimen having a notch in its periphery. He concluded that the thermal conductivity played a key role in determining the width of the shear band. On the other hand Wu and Freund[13], by using a different material model, studied wave propagation in an infinite medium and concluded that the thermal conductivity has essentially no effect on the width of a shear band.

Clifton *et al.*[14] used both numerical and perturbation techniques to study the initiation and growth of shear bands. They used a power law model and reported that the thermal conductivity had virtually no effect on their results. They did not compute the band width explicitly. Also the rate of growth of the nonuniformity increased strongly with decreasing strain-rate sensitivity.

Recently, Wright and Batra[15–17] and Batra[18] described the results of computations that simulate the formation of a shear band from a local temperature inhomogeneity in simple and dipolar materials. The constitutive relation was derived by modifying the dipolar theory of Green *et al.*[19] to include rate effects. For simple materials this constitutive relation reduces to one that is very similar to that proposed by Litonski[7] and Lindholm and Johnson[10]. Whereas Litonski, and Lindholm and Johnson suggested constitutive relations valid for simple shearing deformation of a ductile material, that proposed by Wright and Batra is easily amenable to a general state of stress. Wright and Batra[15–17] and Batra[18] studied the simple shearing of a block made of an isotropic and viscoplastic material and perturbed the homogeneous solution by adding a temperature bump just prior to the occurrence of the peak stress. The stress field was calculated so that every material point was on the yield surface corresponding to its new temperature when all other variables were held fixed. The full set of non-linear coupled governing equations was solved numerically. In Ref. [18] Batra used a similar method to study the interaction among shear bands in simple and dipolar materials.

Herein, for simple materials, we study the effect of various material parameters on the initiation and growth of adiabatic shear bands by adding the temperature perturbation in the configuration when the body just starts deforming plastically. Since this point is far from the peak in the stress–strain curve, our results should reflect the dependence of the rate of growth of the perturbation upon the material parameter being changed. We should add that the complete set of coupled non-linear equations are solved numerically by the Galerkin–Crank–Nicolson method. The computed results show that for the problems studied in which the non-dimensional thermal length varied from 0 to 0.063, the thermal conductivity has no noticeable effect on the strain at which the shear strain localization occurs. In all but one of the cases studied, the stress–strain curve had a peak in it and a narrow region near the center eventually deformed very rapidly with the rest of the material essentially not deforming at all. For the exceptional case noted earlier, the combination of the values of material parameters was such that the stress–strain curve had no peak in it. In this case no localization of deformation occurred even when the amplitude of the initial temperature perturbation was increased to three times its value for other cases. This seems to confirm that the peaking out of stress is a necessary condition for the shearing deformation to localize.

FORMULATION OF THE PROBLEM

We study the simple shearing deformations of a semi-infinite, isotropic and viscoplastic body bounded by the planes $Y = \pm H$ and consider deformation fields of the type

$$x = X + u(Y, t), \qquad y = Y, \qquad z = Z, \qquad \theta = \theta(Y, t). \tag{1}$$

Thus, with respect to a rectangular Cartesian set of axes, (x, y, z) denote the current coordinates of a material point that occupied the place (X, Y, Z) in a stress-free reference configuration. The functions u and θ give, respectively, the displacement of the material point in the x-direction and its temperature change from that in the reference configuration. In the absence of body forces and external sources of heat, the balance of linear momentum and internal energy may be written as

$$\rho \ddot{u} = s_{,y} \tag{2}$$

$$\rho \dot{e} = s\dot{u}_{,y} - q_{,y}. \tag{3}$$

Here ρ is the mass density which stays constant since the deformations considered are isochoric and the effect of temperature changes on the mass density is being neglected, s is the shearing stress in the x-direction on a plane $y = \text{constant}$, e is the specific internal energy, q is the heat flux, a superimposed dot indicates material time derivative, and a comma followed by y signifies partial differentiation with respect to y. We assume that the shear strain has an additive decomposition

$$\gamma \equiv u_{,y} = \gamma_e + \gamma_p \tag{4}$$

and that a loading or yield function f exists such that

$$f(s, \theta, \dot{\gamma}_p) = \kappa \tag{5}$$

where f is a monotonically decreasing function in $\dot{\gamma}_p$ and κ is a measure of the work hardening of the material. The criterion for elastic and plastic loading is

$$f(s, \theta, 0) \leqslant \kappa, \quad \text{elastic} \tag{6}$$

$$f(s, \theta, 0) > \kappa, \quad \text{plastic.} \tag{7}$$

In the latter case, the sign of $\dot{\gamma}_p$ is the same as that of s and its absolute value can be found uniquely from eqn (5) because of the assumed monotonicity of f. The reader is referred to Wright and Batra[15, 17] for further discussion of the yield surface.

Here we make the following choice of constitutive functions

$$\rho e = \tfrac{1}{2}\mu\gamma_e^2 + \rho c_v \theta \tag{8}$$

$$q = -k\theta_{,y} \tag{9}$$

$$\kappa = \kappa_0\left(1 + \frac{\psi}{\psi_0}\right)^n \tag{10}$$

$$\kappa\dot{\psi} = s\dot{\gamma}_p \tag{11}$$

$$f = s/(1 - a\theta)(1 + b\dot{\gamma}_p)^m \tag{12}$$

where μ is a constant shear modulus, c_v is the specific heat at constant volume, k is the thermal conductivity, ψ is the plastic strain in a slow isothermal reference test for which the stress–strain curve (neglecting elastic strains) is given by eqn (10), parameter a describes the thermal softening of the material and material parameters b and m give its strain-rate sensitivity. From eqn (8) it follows by using standard thermodynamic arguments [17] that

$$s = \mu\gamma_e. \tag{13}$$

Therefore

$$\dot{s} = \mu(\dot{\gamma} - \dot{\gamma}_p). \tag{14}$$

Before stating the initial and boundary conditions we introduce non-dimensional variables (indicated by superimposed bars in eqn (15)) as follows:

$$
\begin{array}{lllll}
y = H\bar{y}, & u = H\bar{u}, & s = \kappa_0\bar{s}, & \theta = \dfrac{\kappa_0}{\rho c_v}\,\bar{\theta} \equiv \theta_0\bar{\theta}, & \\[2ex]
t = \dfrac{1}{\dot{\gamma}_0}\,\bar{t}, & \gamma = \bar{\gamma}, & \kappa = \kappa_0\bar{\kappa}, & \psi = \bar{\psi}, & \bar{v}H\dot{\gamma}_0 = v, \\[2ex]
\bar{a} = a\theta_0, & \bar{b} = b\dot{\gamma}_0, & \bar{\rho} = \rho H^2\dot{\gamma}_0^2/\kappa_0, & \bar{k} = k/(\rho c_v\dot{\gamma}_0 H^2). &
\end{array}
\tag{15}
$$

Here $\dot{\gamma}_0$ is the average strain rate imposed in the problem. Dropping the overbars, the complete set of equations in non-dimensional variables may be written as

$$
\begin{aligned}
\dot{v} &= \frac{1}{\rho}\, s_{,y} \\
\dot{\theta} &= k\theta_{,yy} + s\dot{\gamma}_p \\
s &= \mu(v_{,y} - \dot{\gamma}_p) \\
\dot{\psi} &= s\dot{\gamma}_p \bigg/ \left(1 + \frac{\psi}{\psi_0}\right)^n
\end{aligned}
\tag{16}
$$

$$
\dot{\gamma}_p = \max\left[0, \left\{\left(\frac{s}{(1+\psi/\psi_0)^n(1-a\theta)}\right)^{1/m} - 1\right\}\bigg/ b\right].
$$

Whereas we have assumed that all of the plastic work is converted into heat, some authors (e.g. Sulijoadikusumo and Dillon[20]) assume that only about 90% of the plastic work is transformed into heat. Farren and Taylor[21] found that in tensile experiments on steels, copper and aluminum, the heat rise represented 86.5, 90.5–92 and 95%, respectively, of the plastic work. In eqns (16) v is the particle velocity in the x-direction. The boundary conditions

$$
v(\pm 1, t) = \pm 1, \qquad \theta_{,y}(\pm 1, t) = 0 \tag{17}
$$

ensure that the overall applied strain rate is $\dot{\gamma}_0$ and the deformations are adiabatic. For the initial conditions we take

$$
v(y, 0) = y, \qquad \psi(y, 0) = 0, \qquad \theta(y, 0) = 0.1(1-y^2)^9\, e^{-5y^2} \tag{18a}
$$

$$
s(y, 0) = (1 - a\theta(y, 0))(1+b)^m. \tag{18b}
$$

Thus the initial perturbation in the temperature is introduced when the material just starts deforming plastically and the initial stress distribution is adjusted so that all of the material points are on their corresponding yield surfaces.

We seek solutions of eqns (16)–(18) such that v is antisymmetric in y, and s and θ are symmetric in y. Thus we can study the problem on the domain [0, 1] and replace boundary conditions (17) by

$$
v(0, t) = 0, \qquad \theta_{,y}(0, t) = 0, \qquad v(1, t) = 1, \qquad \theta_{,y}(1, t) = 0. \tag{19}
$$

RESPONSE TO PERTURBATIONS

The details of integrating the governing equations (16) under side conditions (18) and (19) by the Galerkin–Crank–Nicolson method are given in Ref. [18]. The domain [0, 1] was divided into 20 subdomains (finite elements) with nodes at 0, 0.0025, 0.01, 0.0225, 0.04, 0.0625, 0.09, 0.1225, 0.160, 0.2025, 0.2500, 0.3025, 0.3600, 0.4225, 0.4900, 0.5625, 0.6400, 0.7225, 0.8100, 0.9025, 1.0. The uniform time increment $\Delta t = 5 \times 10^{-6}$ was used in the Crank–Nicolson method.

The following values of material parameters that correspond to a typical hard steel were chosen:

$$\begin{array}{llll} \rho = 7860\ \mathrm{kg\ m^{-3}}, & k = 49.216\ \mathrm{W\ m^{-1}\ {}^\circ C^{-1}}, & & \mu = 80\ \mathrm{GPa}, \\ \kappa_0 = 333\ \mathrm{MPa}, & a = 0.00552\,{}^\circ\mathrm{C}^{-1}, & & c_v = 473\ \mathrm{J\ kg^{-1}\ {}^\circ C^{-1}}, \\ m = 0.025, & n = 0.09, & \psi_0 = 0.017, & b = 10^4\ \mathrm{s}. \end{array} \tag{20}$$

For this choice of parameters, $\theta_0 = 89.6$°C. Also we took $\dot{\gamma}_0 = 500\ \mathrm{s}^{-1}$ and $H = 2.58$ mm.

As pointed out by Wright and Batra[15], implicit in eqns (16) are two relative length scales, namely a thermal length $(k/\rho c_v \dot{\gamma}_0 H^2)^{1/2}$ and viscous length $(b/H)(\kappa_0/\rho)^{1/2}$. The effect of a change in these as well as in the values of parameters describing thermal softening, work hardening, and rate hardening of the material is studied. The viscous length was varied by altering the value of the material parameter b while keeping the values of all other parameters unchanged. Figure 1 shows the shear stress, the temperature change and the plastic strain rate at the center vs the time elapsed. Since the average strain rate in the specimen is kept fixed at 500 s^{-1}, the average strain γ_{avg} plotted as abscissa in Fig. 1 and other figures is related to the elapsed time Δt in seconds by $\gamma_{\mathrm{avg}} = 500\ \Delta t$. We note that the shear stress in the specimen was initially nonuniform. However, after a brief interval during which the field variables essentially regain their balance, the shear stress becomes uniform throughout the slab and stays uniform up to the time results plotted here. It is obvious from the stress–strain curves plotted in Fig. 1 that with the increase in the value of b the peak stress increases but this peak occurs at a lower value of average strain. The amount by which the peak moves to the left decreases with every 10 fold increase in the value of b suggesting that eventually an increase in the value of b will not affect the strain at which the peak stress occurs. The central plastic strain rate increases rather slowly first, but begins to increase rapidly as the peak in the stress–strain curve is reached and eventually increases

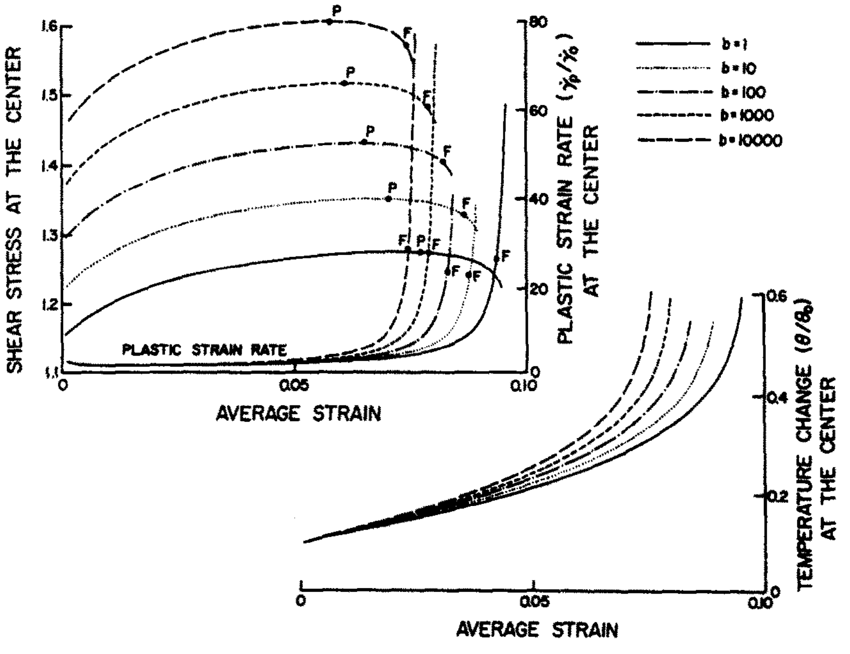

Fig. 1. Effect of the value of material parameter b on the evolution of the central stress, central plastic strain rate and the central temperature.

at an infinite rate when the average strain in the specimen is well past that corresponding to the peak stress. This point is indicated by F on the stress–strain curves. The temperature at the center first increases linearly but soon begins to increase at a faster rate and eventually grows extremely rapidly. Since the shear stress decreases once the peak is passed, the rate of increase of temperature is not as fast as the rate of increase of the plastic strain rate. For the same value of average strain, a higher value of b results in a higher value of θ. We should add that unlike the shear stress, the temperature, plastic strain, plastic strain rate, and particle velocity fields are not uniform throughout the thickness of the slab. Figure 2 depicts the cross-plots of the plastic strain rate, temperature change and the particle velocity for different values of b. The values of time elapsed or the average strain for different curves are not quite the same. This is due to the fact that computed results were printed for identical values of t but the explosive growth in central plastic strain rate occurs at different times. Except for a narrow region near the center, the temperature distribution within the specimen is unaffected by a change in the value of material parameter b. As expected the deformation has localized, and the majority of the block away from the center moves as a rigid body.

Following Wright[22] we define the width of a shear band as twice the distance of the point from the center where the value of the plastic strain rate drops to one-tenth of its maximum value at the center. We note that during the development of the shear band, the plastic strain rate is maximum at the center. At a time later than the one when a dramatic rise in the growth rate of the central plastic strain rate occurs, the value of the plastic strain rate at a node adjoining the center of slab becomes greater than that at the center. This is due to the grid being not as fine as is perhaps required for the proper resolution of the deformation field. Notwithstanding this shortcoming, one can still investigate the effect of the viscous length on the band width. For all five values of the viscous length, the band width came out to be 116 μm. In each case, the central plastic strain rate had reached a value of 80 times the applied average strain rate of 500 s^{-1}. Numerical experiments with a mesh that was finer near the center yielded the same value of the band width and gave a maximum value of the plastic strain rate at the center. We are currently developing a computer code that will refine the mesh adaptively and give a much better resolution of the deformation fields near the center of the slab.

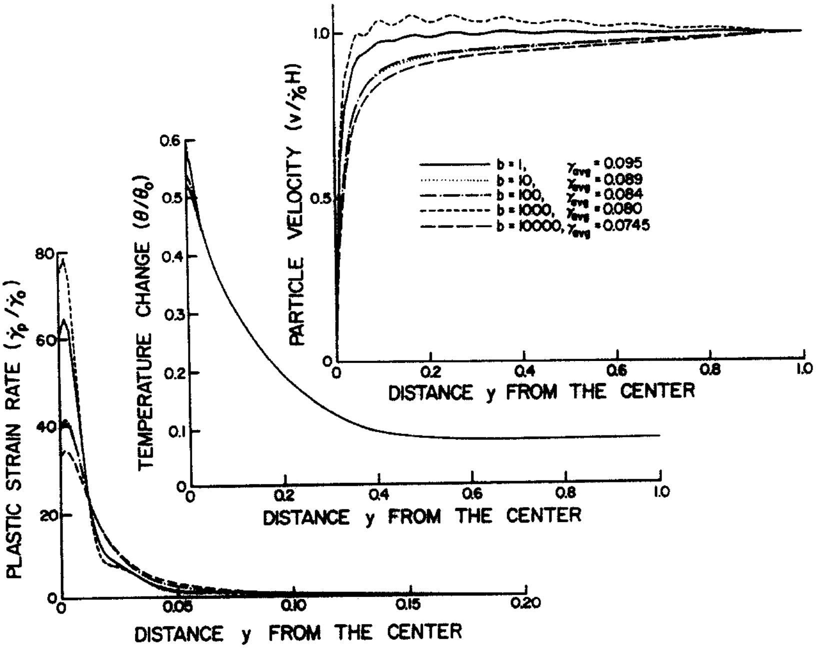

Fig. 2. Effect of the value of material parameter b on the distribution of particle velocity, temperature change and plastic strain rate within the specimen.

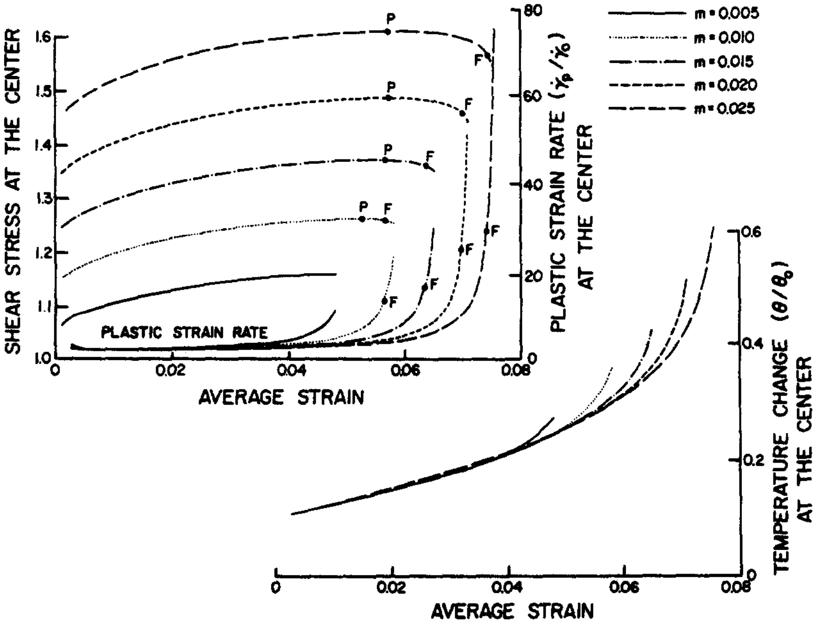

Fig. 3. Stress–strain curves and the evolution of the central plastic strain rate and temperature for different values of *m*.

Another way to alter viscous effects in the materials is to keep *b* fixed but change the rate sensitivity exponent *m*. The effect of this change in the value of *m* is depicted in Figs 3 and 4. Whereas an increase in the value of *m* from 0.005 to 0.015 resulted in higher values of the critical strains at which the peak P in the stress–strain curve occurs, subsequent increases in the value of *m* hardly changed the critical strain. However, the difference between the value of the average strains corresponding to point F when the explosive growth in the central plastic strain rate occurs and the point P increases with *m*. Our numerical results agree with the analytical results of Staker[3] and Clifton *et al.*[14] if we restrict ourselves to $m \geq 0.015$, a value typical for many metals. Clifton *et al.*[14] also noted

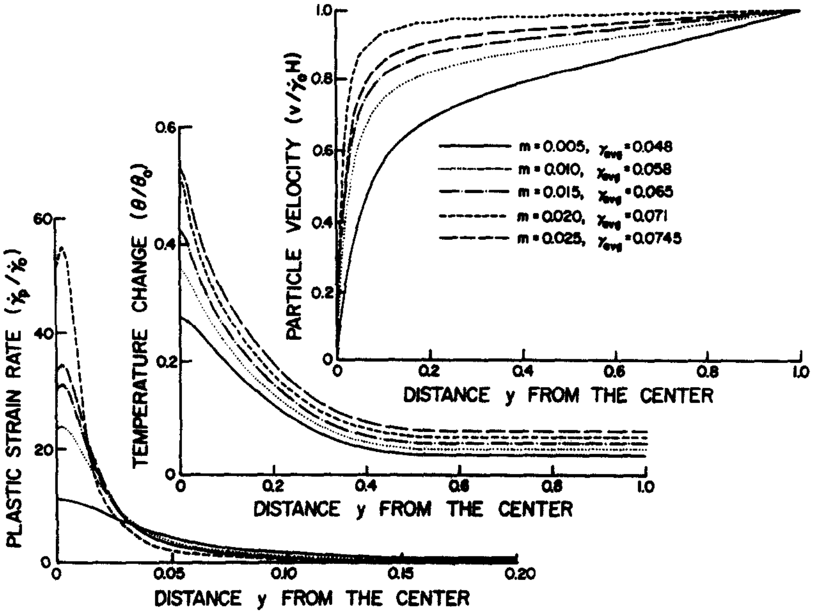

Fig. 4. Distribution of the temperature, particle velocity and plastic strain rate in the specimen for different values of *m*.

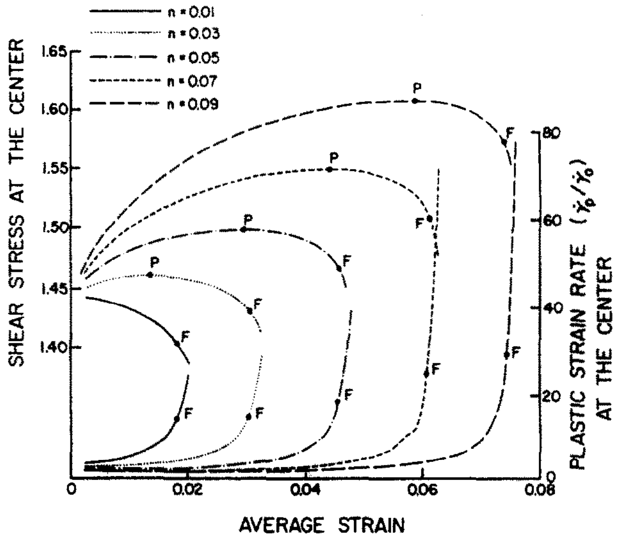

Fig. 5. Stress–strain curves and the evolution of the central plastic strain rate for different values of *n*.

that even though the critical strain may be insensitive to the value of *m*, subsequent growth of the instability will be affected by its value. At early times, the central temperature is unaffected by *m*. Curves representing the evolution of the central temperature more or less coincide until the temperature at the center begins a sharp rise. This behavior differs from that when the values of *b* were increased. Figure 4 depicts the distribution of the plastic strain rate, temperature and particle velocity through the thickness of the slab. Note that these curves do not correspond to the time when the shear band had fully developed in each case. Achieving that goal would have required sorting through a tremendous amount of computer output.

Figures 5 and 6 show results for different values of the strain-hardening exponent *n*. An increase in the value of *n* increases the strain at which the peak P in the stress–strain curve occurs and also the value of the strain at which the explosive growth in the central plastic strain rate occurs. Whereas Bai[5] and Staker[3] showed that the critical strain is proportional to *n*, our computed values of the critical strain divided by *n* gave 8.67, 11.4, 12.14, and 12.67 for $n = 0.03$, 0.05, 0.07, and 0.09, respectively. They assumed a parabolic type $(\gamma_p)^n$ hardening rule and we have represented this effect by $(1+\psi/\psi_0)^n$. Since $\psi_0 \ll 1$, our criterion will increase the flow stress more than the simple parabolic hardening rule will for the same amount of plastic deformation and identical values of *n*. In Fig. 6 are plotted the central temperature vs time or average strain, and the distribution of the particle velocity, temperature and plastic strain rate within the specimen. Again these plots of quantities vs the distance from the center are at different stages of the shear band development for different values of *n*. These depict that qualitatively there is no change in the way various field variables evolve in the specimen as the strain-hardening exponent is increased.

In Fig. 7 are plotted the shear stress at the center, the central plastic strain rate and the central temperatures vs the average strain for three different values of the thermal softening coefficient *a*. For $a = 0.000552$, no peak in the stress–strain curve occurred for strains up to 35%, and the central plastic strain rate grew at a snail's pace, the central temperature increased linearly with average strain and the particle velocity (cf. Fig. 8) had a linear variation through the thickness of the specimen. The temperature was slightly higher at the center than it was at the edge. To see if the increase in the amplitude of the temperature perturbation given by eqn (18a) would result in shear-strain localization, two more cases with the central amplitudes equal to 0.2 and 0.3 were tried. In neither case did the deformation localize. When similar numerical experiments were conducted with $a = 0.00552$, the deformation localized near the center at values of strain well below the

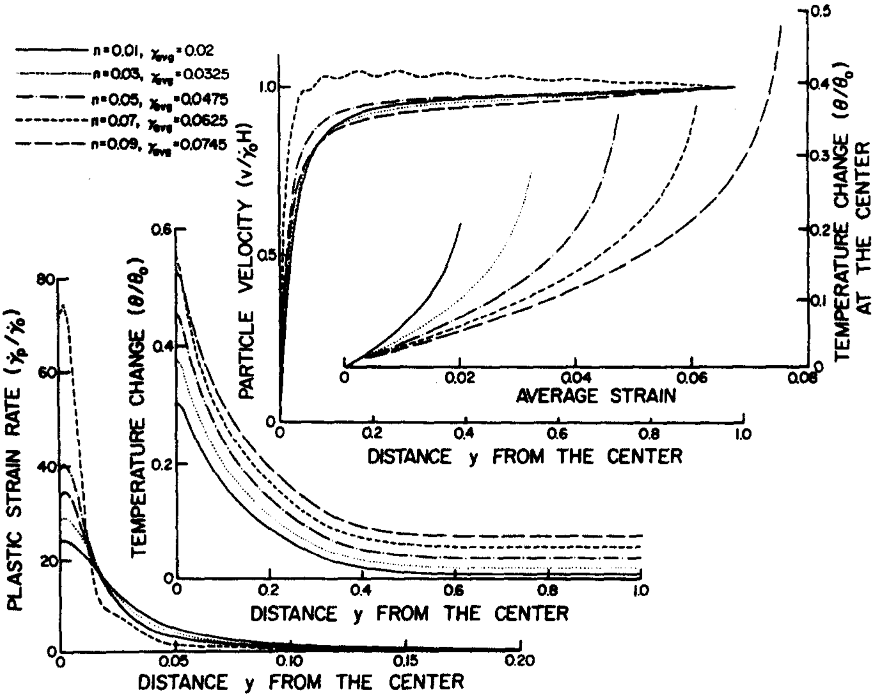

Fig. 6. Temperature change vs average strain and the distribution of the temperature change, plastic strain rate and particle velocity within the slab for different values of n.

ones at which the peak stress occurred. This supports the viewpoint that the existence of the peak in the stress–strain curve is a necessary condition for the deformation to localize.

The expressions for the critical strain derived by Staker[3] and Bai[5] imply that the critical strain is inversely proportional to the thermal softening coefficient a. When we halved the value of a from 0.005552 to 0.002776, the peak in the stress–strain curve occurred at an average strain of 0.0551 instead of 0.15. Whereas we have solved a complete set of equations both Staker and Bai approximated the change in temperature caused by plastic working. As in the other cases studied, the dramatic growth in the central plastic strain rate occurs at a value of strain well past the peak in the stress–strain curve. The width of the shear band is hardly affected by the value of the thermal softening coefficient a provided that the deformation does localize.

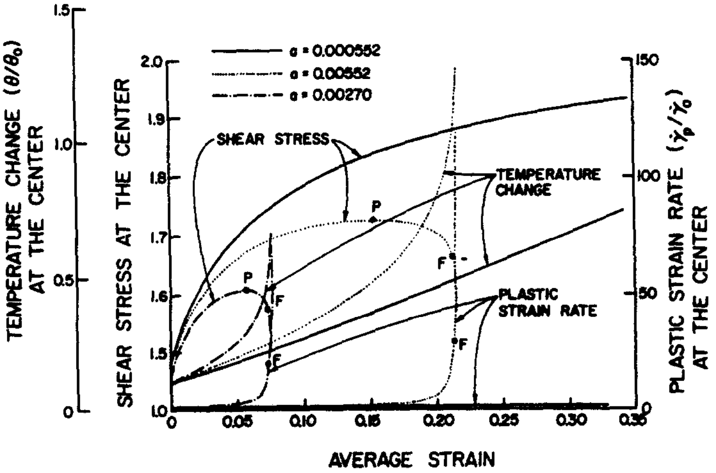

Fig. 7. Effect of the value of the thermal softening coefficient a on the growth of the central stress, plastic strain rate and temperature.

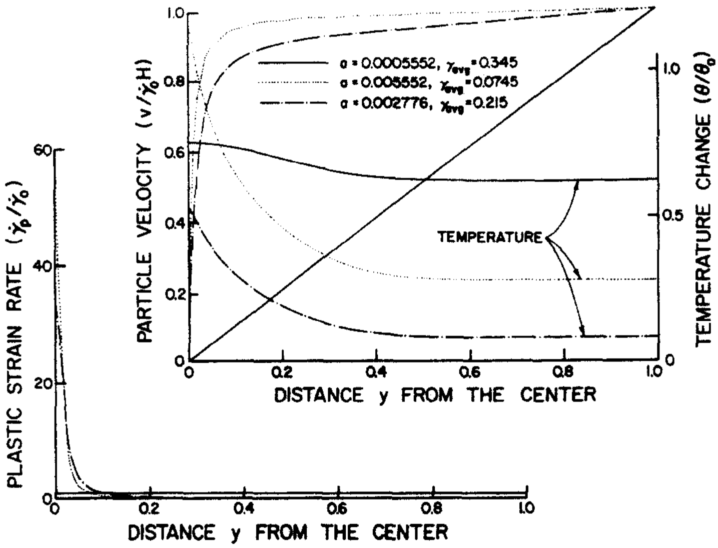

Fig. 8. Variation of the particle velocity, temperature and plastic strain rate within the specimen for different values of a.

Finally we investigated the effect of the thermal length by changing the value of the thermal conductivity k. We note that for the values of ρ, $\dot{\gamma}_0$ and H given in eqns (20), the non-dimensional thermal length decreases from 0.0631 to 0 when the values of thermal conductivity k are changed from 49.216 to 0. For values of k in this range, the stress–strain curves, plotted in Fig. 9, up to the peak stress are unaffected. However, beyond this peak the drop in the stress is slightly affected by the value of the thermal conductivity. Also the strain at which the explosive growth in the central plastic strain rate occurs increases slightly with an increase in the value of k. In Fig. 10 are plotted the variations of the plastic strain rate, temperature and particle velocity in the specimen. Again qualitatively there is no difference in these plots when the thermal conductivity is varied.

For all four values of the thermal length used, the band width came out to be 116 μm. In each case, the central plastic strain rate had reached a value of 80 times the applied strain rate. These results are in agreement with those of Wu and Freund[13] but disagree with the conclusions drawn by Merzer[11]. Note that the constitutive relation and the method of

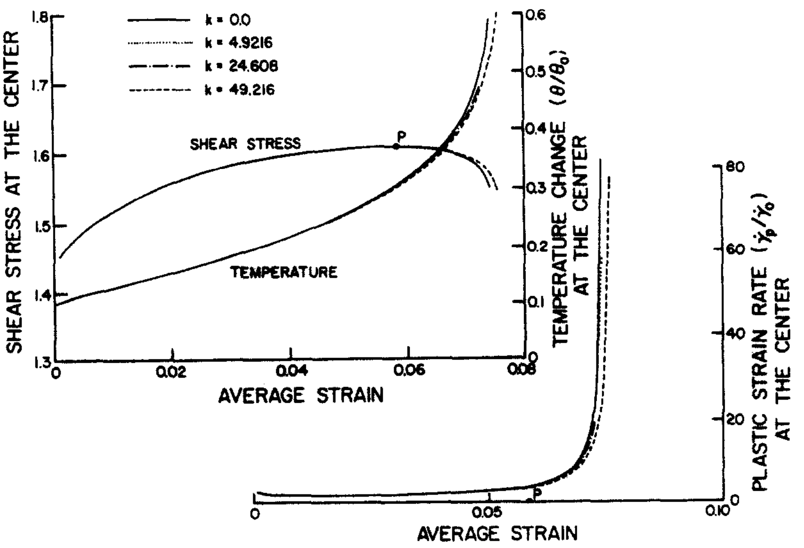

Fig. 9. Effect of the thermal conductivity on the growth of the central shear stress, temperature and the plastic strain rate.

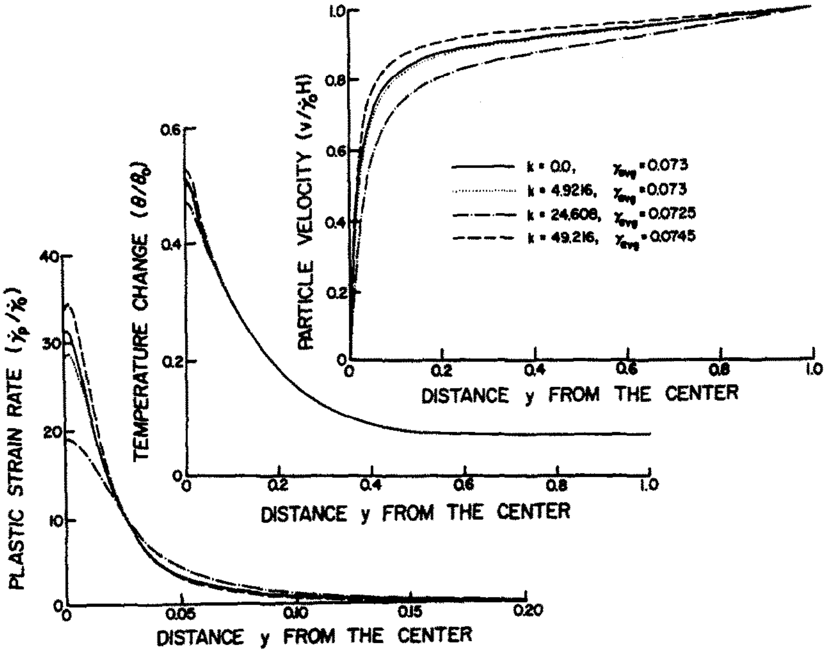

Fig. 10. Distribution of the plastic strain rate, temperature change and the particle velocity in the specimen at four different values of thermal conductivity.

studying the shear band development used herein are different from those employed by Merzer, and Wu and Freund.

CONCLUSIONS

The problem of shear strain localization in simple viscoplastic materials has been studied by using a constitutive relation proposed earlier by Wright and Batra[15]. A shear band is presumed to have formed if the addition of a temperature bump at the center of the specimen in the configuration in which it just deforms plastically results in the localization of the deformation. The complete set of coupled non-linear equations is integrated numerically by using the Galerkin–Crank–Nicolson method.

These numerical experiments reinforce the belief that the existence of a peak in the stress–strain curve is a necessary condition for the shear band to develop. The non-dimensional thermal length with values between 0 and 0.063 has little effect on the critical strain at which the peak in the stress–strain curve occurs, the strain at which the plastic strain rate at the center begins an extremely rapid rise and the width of the band. The critical strain did not come out to be inversely proportional to the thermal softening parameter as has been approximated in some theoretical studies. Even though values of the rate-hardening exponent m greater than 0.015 did not increase the value of the critical strain, the strains at which dramatic growth in the band development occurs did increase with m. Thus from a practical viewpoint, higher values of the strain-rate hardening exponent m, the viscous length and the strain hardening exponent n would delay the development of a shear band.

Finally we note that conclusions drawn herein are strictly applicable to the constitutive model used.

Acknowledgements—This work was supported by the ARO contract DAAG 29-85-K-0238 to the University of Missouri–Rolla.

REFERENCES

1. C. Zener and J. H. Hollomon, Effect of strain rate upon plastic flow of steel. *J. Appl. Phys.* **15**, 22 (1944).
2. R. F. Recht, Catastrophic thermoplastic shear. *J. Appl. Mech.* **31**, 189 (1964).
3. M. R. Staker, The relation between adiabatic shear instability strain and material properties. *Acta Metall.* **29**, 683 (1981).

4. R. J. Clifton, Adiabatic shear in material response to ultrahigh loading rates. NRC National Material Advisory Board (U.S.) Report NMAB-356 (Edited by W. Herrmann *et al.*), Washington, DC (1980).
5. Y. L. Bai, A criterion for thermoplastic shear instability. In *Shock Waves and High Strain-rate Phenomenon in Metals* (Edited by M. A. Meyers and L. E. Murr), pp. 277–284. Plenum Press, New York (1981).
6. T. J. Burns, Approximate linear stability analysis of a model of adiabatic shear band formation. *Q. Appl. Math.* **43,** 65 (1985).
7. J. Litonski, Plastic flow of a tube under adiabatic torsion. *Bull. Acad. Pol. Sci.* **25,** 7 (1977).
8. L. S. Costin, E. E. Crisman, R. H. Hawley and J. Duffy, On the localization of plastic flow in mild steel tubes under dynamic torsional loading. *Inst. Phys. Conf.* Ser. No. 47, 90 (1979).
9. G. R. Johnson, J. M. Hoegfeldt, U. S. Lindholm and A. Nagy, Response of various metals to large torsional strains over a large range of strain rates—Part 1: ductile metals. *ASME J. Engng Mater. Tech.* **105,** 48 (1983).
10. U. S. Lindholm and G. R. Johnson, Strain-rate effects in metals at large strain rates. In *Material Behavior under High Stresses and Ultrahigh Loading Rates* (Edited by J. Mexall and V. Weiss), pp. 61–79. Plenum Press, New York (1983).
11. A. M. Merzer, Modelling of adiabatic shear band development from small imperfections. *J. Mech. Phys. Solids* **30,** 323 (1982).
12. S. R. Bodner and Y. Partom, Mechanical properties at high rate of strain. *Inst. Phys. Conf.* Ser. No. 21, 102 (1975).
13. F. H. Wu and L. B. Freund, Deformation trapping due to thermoplastic instability in one-dimensional wave propagation. *J. Mech. Phys. Solids* **32,** 119 (1984).
14. R. J. Clifton, J. Duffy, K. A. Hartley and T. G. Shawki, On critical conditions for shear band formation at high strain rates. *Scripta Metall.* **18,** 443 (1984).
15. T. W. Wright and R. C. Batra, The initiation and growth of adiabatic shear bands. *Int. J. Plasticity* **1,** 205 (1985).
16. T. W. Wright and R. C. Batra, Further results on the initiation and growth of adiabatic shear bands at high strain rates. *J. Phys.* **46,** 323 (1985).
17. T. W. Wright and R. C. Batra, Adiabatic shear bands in simple and dipolar plastic materials. In *Proceedings of the IUTAM Symposium on Macro- and Micro-mechanics of High Velocity Deformation and Fracture*, Tokyo (August 1985).
18. R. C. Batra, The initiation and growth of, and the interaction among adiabatic shear bands in simple and dipolar materials. *Int. J. Plasticity* **3,** 75 (1987).
19. A. E. Green, B. C. McInnis and P. M. Naghdi, Elastic–plastic continua with simple force dipole. *Int. J. Engng Sci.* **6,** 373 (1968).
20. A. U. Sulijoadikusumo and O. W. Dillon, Jr., Temperature distribution for steady axisymmetric extrusion, with an application to Ti–6Al–4V: Part 1. *Thermal Stresses* **2,** 97 (1979); Part 2, *Ibid.* **2,** 113 (1979); Part 3, *Ibid.* **3,** 265 (1979).
21. W. S. Farren and G. I. Taylor, The heat developed during plastic extrusion of metal. *Proc. R. Soc.* **A107,** 422 (1925).
22. T. W. Wright, Some aspects of adiabatic shear bands. In *Metastability and Incompletely Posed Problems* Edited by S. Antman, J. L. Ericksen, D. Kinderlehrer and I. Müller), pp. 353–372. Springer, Berlin (1987).